Chinese Chemical Letters 34 (2023) 107809

Contents lists available at ScienceDirect

Chinese Chemical Letters

journal homepage: www.elsevier.com/locate/cclet

CO hydrogenation on stepped Cu and CuZn alloy surfaces: Competition between methanol synthesis and methanation pathways

Xuanye Chen [a,b], Wenhua Zhang [a,*], Weixin Huang [a,*]

[a] School of Chemistry and Materials Science, University of Science and Technology of China, Hefei 230026, China
[b] Research Institute of Applied Chemistry, Jiangxi Academy of Sciences, Nanchang 330096, China

ARTICLE INFO

Article history:
Received 19 August 2022
Revised 5 September 2022
Accepted 6 September 2022
Available online 12 September 2022

Keywords:
Theoretical calculation
Reaction mechanism
Structure-activity relation
Facet effect
Defect

ABSTRACT

Comprehensive fundamental understanding of CO hydrogenation reactions over Cu and ZnCu alloy surfaces is of great importance. Herein, we report a comparative DFT calculation study of elementary surface reaction network of CO hydrogenation reactions on stepped Cu(211), Cu(611), ZnCu(211) and ZnCu(611) surfaces. On ZnCu(211) and ZnCu(611) surfaces, the energetic favorable reaction path of CO hydrogenation reaction follows $CO^* \rightarrow HCO^* \rightarrow H_2CO^* \rightarrow H_3CO^* \rightarrow CH_3OH^* \rightarrow CH_3OH$ with H_3CO^* hydrogenation as the rate-limiting step and proceeds more facilely on ZnCu(611) surface than on ZnCu(211) surface. On Cu(211) and Cu(611) surfaces, the energetic favorable reaction path of CO hydrogenation reaction follows $CO^* \rightarrow HCO^* \rightarrow HCOH^* \rightarrow H_2COH^* \rightarrow H_3COH^* \rightarrow CH_3^* \rightarrow CH_4^* \rightarrow CH_4$ with H_2COH^* hydrogenation as the rate-limiting step and proceeds more facilely on Cu(611) than on Cu(211). The key difference of CO hydrogenation reaction on ZnCu alloy surface and Cu is that the resulting CH_3OH^* species desorbs to produce CH_3OH on ZnCu alloy but undergoes H^*-assisted decomposition to CH_3^* and eventually to CH_4 on Cu surface. These results successfully unveil elementary surface reaction networks and structure sensitivity of Cu and ZnCu alloy-catalyzed CO hydrogenation reactions.

Syngas, a mixture of CO and H_2, is widely used as the reactant to produce a variety of organic chemicals, which depends on the used catalysts. Fundamental understanding of catalytic CO hydrogenation reactions is of great importance, but meanwhile, has remained as a long-standing challenge due to the ultrahigh complexity. Theoretical calculations have demonstrated great capacity in fundamentally studying complex catalytic CO hydrogenation reactions [1,2].

Cu-based catalysts have been widely used to catalyze CO hydrogenation reactions either to methanol or to methane, and $Cu/ZnO/Al_2O_3$ catalyst is the commercial catalyst for CO hydrogenation to methanol [3,4]. This has inspired extensive fundamental investigations of CO hydrogenation reactions on Cu-based surfaces, but arguments still exist whether the Cu-ZnO interface or the CuZn alloy is the active site for catalyzing CO hydrogenation to methanol reaction [5–9]. Recently, both experimental and theoretical calculation studies showed the *in-situ* formed CuZn alloys in $Cu/ZnO/Al_2O_3$ catalysts under CO hydrogenation reaction conditions as the active structure, whose formation is preferred at stepped Cu sites and whose catalytic performance is sensitive to the Cu structure [10–12]. However, comprehensive studies of elementary surface reaction networks of CO hydrogenation reactions to both methanol and methane on stepped Cu and CuZn alloy surfaces have been few. Cu(211) and Cu(611) stepped facets are very common on the low-indexed Cu(111) and Cu(100) surfaces, respectively. In this Letter, we report a comparative DFT calculation study of elementary surface reaction networks of CO hydrogenation on stepped Cu(211), Cu(611), ZnCu(211) and ZnCu(611) surfaces. The results demonstrate surface structure-sensitive catalytic activity and reaction mechanisms.

DFT calculations were carried out using the Vienna ab-initio simulation package (VASP) [13,14] using the projector-augment wave (PAW) method [15]. The nonlocal exchange correlation energy was performed via the generalized gradient approximation (GGA) and PBE functional [16,17]. 11-layer slab with (1×4) surface cell and 22-layer slab with (1×2) surface cell were performed to simulate stepped surface Cu(211) and Cu(611). A (1×4)-11-layer Cu(211) slab and a (1×2)-22-layer Cu(611) slab with 1/4 Cu substituted by Zn on the step edge, denoted as ZnCu(211) and ZnCu(611), were used to simulate CuZn alloy [18]. The adsorption energies (E_{ads}) was calculated at the most stable configuration as $E_{ads} = E_{ads/sub} - E_{ads} - E_{sub}$, in which $E_{ads/sub}$, E_{ads} and

* Corresponding authors.
E-mail addresses: whhzhang@ustc.edu.cn (W. Zhang), huangwx@ustc.edu.cn (W. Huang).

https://doi.org/10.1016/j.cclet.2022.107809
1001-8417/

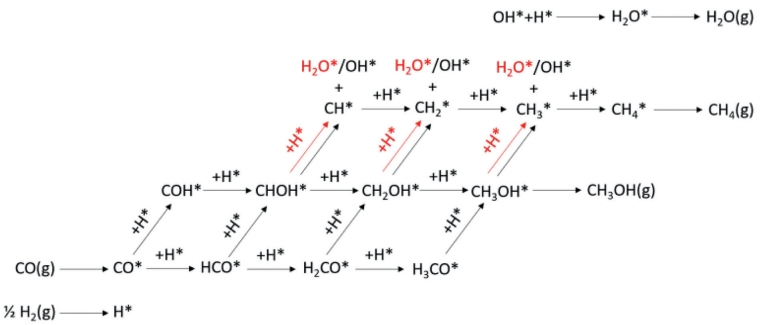

Fig. 1. Calculated elementary surface reaction network of CO hydrogenation reactions on Cu and CuZn alloy surfaces. The red arrows represent the elementary surface reactions of $CH_nOH^* + H^* \rightarrow CH_n^* + H_2O^*$ ($n = 1, 2, 3$).

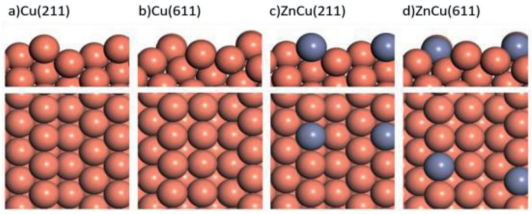

Fig. 2. Side and top views of optimized structures of stepped Cu(211), Cu(611), ZnCu(211) and ZnCu(611) surfaces.

E_{sub} are the energy of the optimized adsorption system of adsorbate and substrate, adsorbate in the gas phase, and the clean substrate, respectively. All transition states (TSs) were located by the force reversed method [19] and climbing-image nudged elastic band method (CINEB) [20,21]. A value of $U-J = 4.7$ eV was used for the correction of the on-site Coulomb repulsion of 3d electrons of Zn atoms [22–24].

Fig. 1 illustrates calculated elementary surface reaction network of CO hydrogenation reactions on Cu and CuZn alloy surfaces during our theoretical calculations. Direct CO dissociation on Cu surfaces was reported to exhibit large barriers [25,26], thus only H-assisted CO activation paths were considered, including $CO^* + H^* \rightarrow HCO^*$ and $CO^* + H^* \rightarrow COH^*$. The elementary surface reaction network consists of competing elementary surface reactions between $H_nCO^* + H^* \rightarrow H_{n+1}CO^*$ and $H_nCO^* + H^* \rightarrow CH_nOH^*$ ($n = 0, 1, 2$), competing elementary surface reactions among $CH_nOH^* \rightarrow CH_n^* + OH^*$, $CH_nOH^* + H^* \rightarrow CH_n^* + H_2O^*$ ($n = 1, 2, 3$) and $CH_nOH^* + H^* \rightarrow CH_{n+1}OH^*$ ($n = 1, 2$), elementary surface reactions of $CH_n^* + H^* \rightarrow CH_{n+1}^*$ ($n = 1, 2, 3$), adsorption of CO and H_2, and desorption of CH_3OH^*, CH_4^* and H_2O^*.

Fig. 2 presents the optimized structures of stepped Cu(211), Cu(611), ZnCu(211) and ZnCu(611) surfaces. Adsorptions of surface intermediates included in Fig. 1 on Cu and ZnCu surfaces were calculated. The optimized adsorption configurations are shown in Fig. S1 (Supporting information) and the corresponding adsorption energies are summarized in Table S1 (Supporting information). Cu(611) and ZnCu(611) bind surface intermediates more strongly than Cu(211) and ZnCu(211), respectively, consistent with the fact that a more open surface with more coordination-unsaturated surface atoms is more reactive. Meanwhile, Cu(211) and Cu(611) bind surface intermediates more strongly than ZnCu(211) and ZnCu(611), respectively, suggesting that alloying with Zn weakens the reactivity of Cu surface. CH_4 adsorption energies on Cu(211), Cu(611), ZnCu(211) and ZnCu(611) surfaces are all within −0.2 eV, however, CH_3OH adsorption energy decreases from −0.67 eV on Cu(211) to −0.32 eV on ZnCu(211) and from −0.83 eV on Cu(611) to −0.56 eV on ZnCu(611), and H_2O adsorption energy decreases from −0.51 eV on Cu(211) to −0.39 eV on ZnCu(211) and from −0.68 eV on Cu(611) to −0.48 eV on ZnCu(611). Thus, desorption of produced CH_3OH^* and H_2O^* species on ZnCu alloy surfaces is much easier than on corresponding Cu surfaces.

Activation energy (E_a) and reaction energy (E_r) of elementary surface reactions shown in Fig. 1 were also calculated. The calculated E_a and E_r are summarized in Table 1 and the optimized configurations of involved transition states are shown in Figs. S2–S4 (Supporting information). The E_a and E_r of H_2 dissociation were calculated to be 0.11 and −0.46 eV on Cu(211), 0.06 and −0.57 eV on Cu(611), 0.12 and −0.35 eV on ZnCu(211), and 0.08 and −0.44 eV on ZnCu(611), respectively. Therefore, H_2 dissociation is facilitated both kinetically and thermodynamically on a more open Cu surface. Meanwhile, alloying with Zn slightly increases the barrier and decreases the reaction energy of H_2 dissociation on the Cu surface.

The E_r of $CO^* + H^* \rightarrow HCO^*$ and $CO^* + H^* \rightarrow COH^*$ reactions were calculated as 0.24 and 2.08 eV on Cu(211), 0.31 and 1.90 eV on Cu(611), 0.42 and 1.69 eV on ZnCu(211), and 0.40 and 1.71 eV on ZnCu(611), respectively. Meanwhile, the E_a of $CO^* + H^* \rightarrow HCO^*$ reaction were calculated as 0.67, 0.60, 0.76 and 0.69 eV on Cu(211), Cu(611), ZnCu(211) and ZnCu(611), respectively. This indicates that the E_a of $CO^* + H^* \rightarrow COH^*$ reaction on Cu and ZnCu surfaces is much larger than that of $CO^* + H^* \rightarrow HCO^*$ and those of other elementary surface reactions. Thus, the $CO^* + H^* \rightarrow COH^*$ reaction does not likely occur under CO hydrogenation reactions over Cu and ZnCu alloy surfaces.

The E_r/E_a of $HCO^* + H^* \rightarrow CHOH^*$ and $HCO^* + H^* \rightarrow H_2CO^*$ are 0.20/0.42 eV and −0.13/0.51 eV on Cu(211) and 0.21/0.27 eV and −0.24/0.57 eV on Cu(611), respectively. Thus $HCO^* + H^* \rightarrow CHOH^*$ is endothermic on Cu surfaces whereas $HCO^* + H^* \rightarrow H_2CO^*$ is exothermic; however, $HCO^* + H^* \rightarrow CHOH^*$ exhibits a smaller barrier than $HCO^* + H^* \rightarrow H_2CO^*$, the difference of which is 0.09 eV on Cu(211) and 0.30 eV on Cu(611). The E_r/E_a of $H_2CO^* + H^* \rightarrow CH_2OH^*$ and $H_2CO^* + H^* \rightarrow H_3CO^*$ are −0.31/0.39 eV and −0.86/0.27 eV on Cu(211) and −0.14/0.33 eV and −0.77/0.18 eV on Cu(611), respectively, suggesting that $H_2CO^* + H^* \rightarrow H_3CO^*$ is preferred both thermodynamically and kinetically over $H_2CO^* + H^* \rightarrow CH_2OH^*$. The E_r/E_a of $H_3CO^* + H^* \rightarrow CH_3OH^*$ are −0.11/0.91 eV on Cu(211) and 0.07/0.79 eV on Cu(611).

The E_r/E_a of $CHOH^* + H^* \rightarrow CH_2OH^*$, $CHOH^* + H^* \rightarrow CH^* + H_2O^*$ and $CHOH^* \rightarrow CH^* + OH^*$ are −0.84/0.37 eV, 0.52/1.37 eV and 0.66/1.41 eV on Cu(211), and −1.02/0.20 eV, 0.35/1.16 eV and 0.40/1.28 eV on Cu(611), respectively. Meanwhile, the E_r/E_a of $CH_2OH^* + H^* \rightarrow CH_3OH^*$, $CH_2OH^* + H^* \rightarrow CH_2^* + H_2O^*$ and $CH_2OH^* \rightarrow CH_2^* + OH^*$ are −0.23/0.99 eV, 0.46/1.08 eV and 0.38/1.34 eV on Cu(211), and −0.05/0.88 eV, 0.28/0.95 eV and 0.42/1.09 eV on Cu(611), respectively. Thus, $CH_nOH^* + H^* \rightarrow CH_{n+1}OH^*$ ($n = 1, 2$) is preferred both thermodynamically and kinetically over $CH_nOH^* + H^* \rightarrow CH_n^* + H_2O^*$ and $CH_nOH^* \rightarrow CH_n^* + OH^*$, particularly for the $CHOH^*$ species.

Table 1
Calculated activation energies (E_a in eV) and reaction energies (E_r in eV) of elementary surface reactions involved in CO hydrogenation on Cu(211), Cu(611), ZnCu(211) and ZnCu (611) surfaces.

Elementary surface reactions	Cu(211)		Cu(611)		ZnCu(211)		ZnCu(611)	
	E_r	E_a	E_r	E_a	E_r	E_a	E_r	E_a
$CO(g)+^*\rightarrow CO^*$	−0.89	/	−1.03	/	−0.78	/	−0.96	/
$CO^*+H^*\rightarrow HCO^*$	0.24	0.67	0.31	0.60	0.42	0.76	0.40	0.69
$CO^*+H^*\rightarrow COH^*$	2.08	/	1.90	/	1.69	/	1.71	/
$HCO^*+H^*\rightarrow CHOH^*$	0.20	0.42	0.21	0.27	0.26	0.85	0.07	0.76
$HCO^*+H^*\rightarrow H_2CO^*$	−0.13	0.51	−0.24	0.57	−0.25	0.69	−0.34	0.66
$CHOH^*+H^*\rightarrow CH_2OH^*$	−0.84	0.37	−1.02	0.20	−0.90	0.44	−0.96	0.29
$CHOH^*+H^*\rightarrow CH^*+H_2O^*$	0.52	1.37	0.35	1.16	0.55	1.48	0.53	1.30
$CHOH^*\rightarrow CH^*+OH^*$	0.66	1.41	0.40	1.28	0.64	1.69	0.47	1.43
$H_2CO^*+H^*\rightarrow CH_2OH^*$	−0.31	0.39	−0.14	0.33	−0.36	0.68	−0.22	0.57
$H_2CO^*+H^*\rightarrow H_3CO^*$	−0.86	0.27	−0.77	0.18	−0.69	0.59	−0.51	0.46
$CH_2OH^*+H^*\rightarrow CH_3OH^*$	−0.23	0.99	−0.05	0.88	−0.20	1.15	−0.31	1.03
$CH_2OH^*+H^*\rightarrow CH_2^*+H_2O^*$	0.46	1.08	0.28	0.95	0.33	1.29	0.45	1.16
$CH_2OH^*\rightarrow CH_2^*+OH^*$	0.38	1.34	0.42	1.09	0.31	1.44	0.52	1.21
$H_3CO^*+H^*\rightarrow CH_3OH^*$	−0.11	0.91	0.07	0.79	0.21	1.02	0.16	0.85
$CH_3OH^*+H^*\rightarrow CH_3^*+H_2O^*$	−0.33	0.43	−0.17	0.35	−0.36	0.81	−0.42	0.67
$CH^*+H^*\rightarrow CH_2^*$	−0.86	0.49	−1.05	0.27	−0.53	0.53	−0.78	0.34
$CH_2^*+H^*\rightarrow CH_3^*$	−1.20	0.34	−1.08	0.12	−0.72	0.56	−0.69	0.38
$CH_3^*+H^*\rightarrow CH_4^*$	−0.42	0.60	−0.54	0.45	−0.36	0.66	−0.39	0.49
$CH_3OH^*\rightarrow CH_3OH(g)+^*$	0.67	/	0.83	/	0.32	/	0.56	/
$CH_4\ ^*\rightarrow CH_4(g)+^*$	0.14	/	0.18	/	0.09	/	0.12	/
$H_2O^*\rightarrow H_2O(g)+^*$	0.51	/	0.68	/	0.39		0.48	

The E_r/E_a of $CH_3OH^*+H^*\rightarrow CH_3^*+H_2O^*$ are −0.33/0.43 eV on Cu(211) and −0.17/0.35 eV on Cu(611), respectively, whereas the E_r of CH_3OH^* desorption is 0.67 and 0.83 eV on Cu(211) and Cu(611), respectively. Thus the CH_3OH^* prefers both thermodynamically and kinetically the reaction of $CH_3OH^*+H^*\rightarrow CH_3^*+H_2O^*$ to produce CH_3^* over the desorption to produce CH_3OH. The E_r/E_a of $CH_3^*+H^*\rightarrow CH_4^*$ are −0.42/0.60 eV on Cu(211) and −0.54/0.45 eV on Cu(611), respectively, and the E_r of CH_4^* desorption is 0.14 and 0.18 eV on Cu(211) and Cu(611), respectively.

The E_r/E_a of $HCO^*+H^*\rightarrow CHOH^*$ and $HCO^*+H^*\rightarrow H_2CO^*$ are 0.26/0.85 eV and −0.25/0.69 eV on ZnCu(211) and 0.07/0.76 eV and −0.34/0.66 eV on ZnCu(611), respectively. The E_r/E_a of $H_2CO^*+H^*\rightarrow CH_2OH^*$ and $H_2CO^*+H^*\rightarrow H_3CO^*$ are −0.36/0.68 eV and −0.69/0.59 eV on ZnCu(211) and −0.22/0.57 eV and −0.51/0.46 eV on ZnCu(611), respectively. Thus, $H_nCO^*+H^*\rightarrow H_{n+1}CO^*$ is preferred both thermodynamically and kinetically over $H_nCO^*+H^*\rightarrow CH_nOH^*$ ($n=1$, 2). The E_r/E_a of $H_3CO^*+H^*\rightarrow CH_3OH^*$ are 0.21/1.02 eV on ZnCu(211) and 0.16/0.85 eV on ZnCu(611).

The E_r/E_a of $CHOH^*+H^*\rightarrow CH_2OH^*$, $CHOH^*+H^*\rightarrow CH^*+H_2O^*$ and $CHOH^*\rightarrow CH^*+OH^*$ are −0.90/0.44 eV, 0.55/1.48 eV and 0.64/1.69 eV on ZnCu(211), and −0.96/0.29 eV, 0.53/1.30 eV and 0.47/1.43 eV on ZnCu(611), respectively. Meanwhile, the E_r/E_a of $CH_2OH^*+H^*\rightarrow CH_3OH^*$, $CH_2OH^*+H^*\rightarrow CH_2^*+H_2O^*$ and $CH_2OH^*\rightarrow CH_2^*+OH^*$ are −0.20/1.15 eV, 0.33/1.29 eV and 0.31/1.44 eV on ZnCu(211), and −0.31/1.03 eV, 0.45/1.16 eV and 0.52/1.21 eV on ZnCu(611), respectively. Thus, $CH_nOH^*+H^*\rightarrow CH_{n+1}OH^*$ ($n=1$, 2) is preferred both thermodynamically and kinetically over $CH_nOH^*+H^*\rightarrow CH_n^*+H_2O^*$ and $CH_nOH^*\rightarrow CH_n^*+OH^*$, particularly for the $CHOH^*$ species.

The E_r/E_a of $CH_3OH^*+H^*\rightarrow CH_3^*+H_2O^*$ are −0.36/0.81 eV on ZnCu(211) and −0.42/0.67 eV on ZnCu(611), respectively, whereas the E_r of CH_3OH^* desorption is 0.32 and 0.56 eV on ZnCu(211) and ZnCu(611), respectively. Thus the CH_3OH^* prefers both thermodynamically and kinetically the desorption to produce CH_3OH over the reaction of $CH_3OH^*+H^*\rightarrow CH_3^*+H_2O^*$ to produce CH_3^*.

Based on the above calculation results, the energetic favorable reaction path of CO hydrogenation reaction follows $CO^*\rightarrow HCO^*\rightarrow CHOH^*\rightarrow CH_2OH^*\rightarrow CH_3OH^*\rightarrow CH_3^*\rightarrow CH_4^*\rightarrow CH_4$ on Cu(211) and Cu(611) surfaces (Fig. 3a). The $CH_2OH^*+H^*\rightarrow CH_3OH^*$ is the rate-limiting step, and its barrier is smaller on Cu(611) (0.88 eV) than on Cu(211) (0.99 eV). Meanwhile, the barriers of $CH_3OH^*+H^*\rightarrow CH_3^*+H_2O^*$ and CH_3OH^* desorption determine the catalytic selectivity of CH_3OH and CH_4, being 0.43 and 0.67 eV on Cu(211) and 0.35 and 0.83 eV on Cu(611), respectively, thus Cu(611) surface should exhibit a higher CH_4 selectivity than Cu(211) surface. Therefore, Cu(611) surface is more active and selective than Cu(211) surface in catalyzing CO hydrogenation reaction to CH_4. However, it is noteworthy that the reaction path of $HCO^*\rightarrow H_2CO^*\rightarrow H_3CO^*\rightarrow CH_3OH^*\rightarrow CH_3^*\rightarrow CH_4^*\rightarrow CH_4$ likely occurs on Cu(211) due to the not much differences between $HCO^*+H^*\rightarrow CHOH^*$ and $HCO^*+H^*\rightarrow H_2CO^*$, but not on Cu(611).

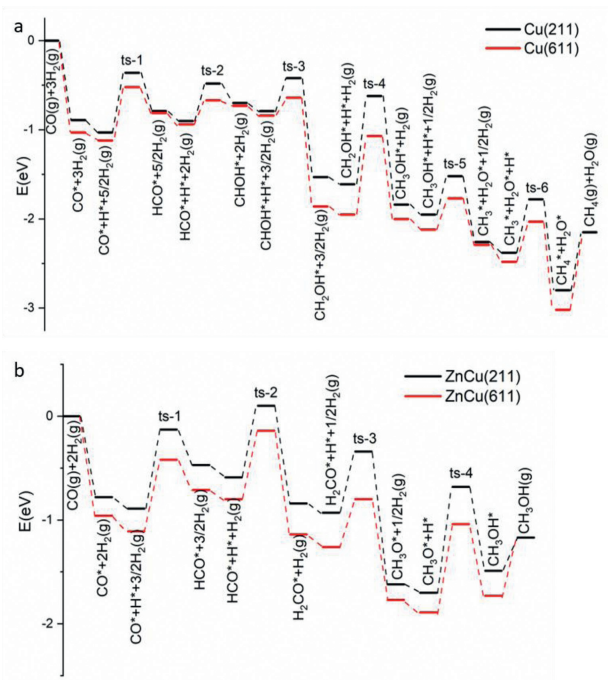

Fig. 3. Energetic favorable reaction path of CO hydrogenation reaction on (a) Cu(211) and Cu(611) surfaces and (b) ZnCu(211) and ZnCu(611) surfaces.

Alloying Cu surface with Zn leads to a larger barrier of $HCO^* + H^* \rightarrow CHOH^*$ than of $HCO^* + H^* \rightarrow H_2CO^*$ and a larger barrier of $CH_3OH^* + H^* \rightarrow CH_3{}^* + H_2O^*$ than CH_3OH^* desorption, thus the energetic favorable reaction path of CO hydrogenation reaction follows $CO^* \rightarrow HCO^* \rightarrow H_2CO^* \rightarrow H_3CO^* \rightarrow CH_3OH^* \rightarrow CH_3OH$ on ZnCu(211) and ZnCu(611) surfaces (Fig. 3b). The $H_3CO^* + H^* \rightarrow CH_3OH^*$ reaction is the rate-limiting step, and its barrier is smaller on ZnCu(611) (0.85 eV) than on ZnCu(211) (1.02 eV). However, the barriers of $CH_3OH^* + H^* \rightarrow CH_3{}^* + H_2O^*$ and CH_3OH^* desorption are 0.81 and 0.32 eV on ZnCu(211) and 0.67 and 0.56 eV on ZnCu(611), respectively. Therefore, ZnCu(611) surface is more active but less selective than ZnCu(211) surface in catalyzing CO hydrogenation reaction to CH_3OH.

In summary, *via* a comparative DFT calculation study of elementary surface reaction network, we demonstrate the energetic favorable reaction path and structure-sensitivity of CO hydrogenation reactions on stepped Cu(211), Cu(611), ZnCu(211) and ZnCu(611) surfaces. CO hydrogenation reaction on Cu(211) and Cu(611) surfaces favorably produces CH_4 following the reaction path of $CO^* \rightarrow HCO^* \rightarrow CHOH^* \rightarrow CH_2OH^* \rightarrow CH_3OH^* \rightarrow CH_3{}^* \rightarrow CH_4{}^* \rightarrow CH_4$. Cu(611) surface is more active and selective than Cu(211) surface. Alloying Cu surface with Zn leads to a larger barrier of $HCO^* + H^* \rightarrow CHOH^*$ than of $HCO^* + H^* \rightarrow H_2CO^*$ and a larger barrier of $CH_3OH^* + H^* \rightarrow CH_3{}^* + H_2O^*$ than CH_3OH^* desorption, resulting in the favorite reaction path of CO hydrogenation reaction on ZnCu(211) and ZnCu(611) surfaces as $CO^* \rightarrow HCO^* \rightarrow H_2CO^* \rightarrow H_3CO^* \rightarrow CH_3OH^* \rightarrow CH_3OH$ to produce CH_3OH. ZnCu(611) surface is more active but less selective than ZnCu(211) surface.

Declaration of competing interest

The authors declare that they have no known competing financial interests or personal relationships that could have appeared to influence the work reported in this paper.

Acknowledgments

This work was financially supported by the National Natural Science Foundation of China (Nos. 91745202, 92145302), the Chinese Academy of Sciences, the Changjiang Scholars Program of Ministry of Education of China.

Supplementary materials

Supplementary material associated with this article can be found, in the online version, at doi:10.1016/j.cclet.2022.107809.

References

[1] W. Chen, R. Pestman, B. Zijlstra, I.A.W. Filot, E.J.M. Hensen, ACS Catal. 7 (2017) 8050–8060.
[2] W. Chen, I.A.W. Filot, R. Pestman, E.J.M. Hensen, ACS Catal. 7 (2017) 8061–8071.
[3] K.C. Waugh, Catal. Today 15 (1992) 51–75.
[4] K. Klier, Adv. Catal. 31 (1982) 243–313.
[5] S. Kuld, et al., Science 352 (2016) 969–974.
[6] F. Studt, et al., ChemCatChem 7 (2015) 1105–1111.
[7] Y. Choi, K. Futagami, T. Fujitani, J. Nakamura, Catal. Lett. 73 (2001) 27–31.
[8] D. Laudenschleger, H. Ruland, M. Muhler, Nat. Commun. 11 (2020) 3898.
[9] N.D. Nielsen, J. Thrane, A.D. Jensen, J.M. Christensen, Catal. Lett. 150 (2020) 1427–1433.
[10] M. Behrens, et al., Science 336 (2012) 893–897.
[11] Z. Zhang, X. Chen, J. Kang, et al., Nat. Commun. 12 (2021) 4331.
[12] Y.F. Shi, P.L. Kang, C. Shang, Z.P. Liu, J. Am. Chem. Soc. 144 (2022) 13401–13414.
[13] G. Kresse, D. Joubert, Phys. Rev. B 59 (1999) 1758–1775.
[14] G. Kresse, J. Furthmuller, Phys. Rev. B 54 (1996) 11169–11186.
[15] P.E. Blochl, Phys. Rev. B 50 (1994) 17953–17979.
[16] J.P. Perdew, Y. Wang, Phys. Rev. B 45 (1992) 13244–13249.
[17] J.P. Perdew, K. Burke, M. Ernzerhof, Phys. Rev. Lett. 77 (1996) 3865–3868.
[18] F. Studt, F. Abild-Pedersen, J.B. Varley, J.K. Nørskov, Catal. Lett. 143 (2013) 71–73.
[19] K.J. Sun, Y.H. Zhao, H.Y. Su, W.X. Li, Theor. Chem. Acc. 131 (2012) 1118–1127.
[20] G. Henkelman, H. Jonsson, J. Chem. Phys. 113 (2000) 9978–9985.
[21] G. Henkelman, B.P. Uberuaga, H. Jonsson, J. Chem. Phys. 113 (2000) 9901–9904.
[22] A. Janotti, C.G. Van de Walle, Phys. Rev. B 76 (2007) 165202–165223.
[23] F. Liao, X.P. Wu, J. Zheng, et al., Catal. Sci. Technol. 6 (2016) 7698–7702.
[24] F. Liao, X.P. Wu, J. Zheng, et al., Green Chem. 19 (2017) 270–280.
[25] X.H. Zhao, Y.W. Li, J.G. Wang, C.F. Huo, J. Fuel Chem. Technol. 39 (2011) 956–960.
[26] G. Jia, L. Ling, R. Zhang, B. Wang, Mol. Catal. 518 (2022) 112071.